Environmental Science & Technology

ARTICLE

pubs.acs.org/est

Modeling Exposure Close to Air Pollution Sources in Naturally Ventilated Residences: Association of Turbulent Diffusion Coefficient with Air Change Rate

Kai-Chung Cheng,* Viviana Acevedo-Bolton, Ruo-Ting Jiang, Neil E. Klepeis, Wayne R. Ott, Oliver B. Fringer, and Lynn M. Hildemann

Civil & Environmental Engineering Department, Stanford University, Stanford, California 94305, United States

Supporting Information

ABSTRACT: For modeling exposure close to an indoor air pollution source, an isotropic turbulent diffusion coefficient is used to represent the average spread of emissions. However, its magnitude indoors has been difficult to assess experimentally due to limitations in the number of monitors available. We used 30−37 real-time monitors to simultaneously measure CO at different angles and distances from a continuous indoor point source. For 11 experiments involving two houses, with natural ventilation conditions ranging from <0.2 to >5 air changes per h, an eddy diffusion model was used to estimate the turbulent diffusion coefficients, which ranged from 0.001 to 0.013 m^2 s^{-1}. The model reproduced observed concentrations with reasonable accuracy over radial distances of 0.25−5.0 m. The air change rate, as measured using a SF_6 tracer gas release, showed a significant positive linear correlation with the air mixing rate, defined as the turbulent diffusion coefficient divided by a squared length scale representing the room size. The ability to estimate the indoor turbulent diffusion coefficient using two readily measurable parameters (air change rate and room dimensions) is useful for accurately modeling exposures in close proximity to an indoor pollution source.

INTRODUCTION

Typically, air pollutant concentrations near an indoor emission source have been estimated using the well-mixed mass balance model (e.g., refs 1−6), which assumes that pollutant emissions become instantaneously, completely well-mixed. Therefore, concentrations are represented as spatially homogeneous within an indoor space but varying with time due to emissions and removal pathways. The indoor time scale for approaching a well-mixed state following release is typically <1 h.[7−10] Thus, this modeling approach will be accurate when the source emission and mixing time scales are much shorter than the duration of exposure.

However, for a source emission period comparable to the exposure time, imperfect mixing becomes important to consider. Exposure will be substantially higher in close proximity to an active source, but this "*proximity effect*" will not be captured by a uniform mixing model.[11−19]

To model the effect of proximity, various mass transfer models have been proposed that use isotropic turbulent diffusion to characterize the mixing of emissions indoors. Analytical solutions of Fick's law have been used to describe turbulent mixing and model indoor concentrations vs distance from a point source that is continuous[20−22] and of short duration.[23] For forced air flow, Scheff et al.[24] used an advection−diffusion equation to predict pollutant transport from indoor point sources. Detailed discussions of these analytical models have been published.[25,26] Another type of approach, random walk theory, has been applied to describe turbulent diffusion transport indoors,[27] using a stochastic Markov chain model to predict the spatial variations in concentration. All these models rely on one empirical parameter—the isotropic turbulent diffusion coefficient (K)—to describe how fast air pollutants disperse with time due to turbulent mixing indoors.

One approach for finding K defines the mixing time as the time at which the coefficient of variation (CV) for all simultaneous measurements drops below 10%. Baughman et al.[7] and Drescher et al.[8] empirically determined mixing times for a pulsed source release in an experimental room under natural and forced ventilation conditions. Klepeis[9] similarly characterized mixing times in two indoor field locations. A recent study,[10] also involving pulsed releases in a chamber, used CV < 20%. With these indoor mixing times, an eddy diffusion model can determine which K gives comparable mixing times.

K can also be estimated by fitting model predictions to measurements at different distances from a source. Scheff et al.[24] measured 1-h-averaged concentrations at nine positions inside a

Received: September 8, 2010
Accepted: March 8, 2011
Revised: February 28, 2011
Published: April 01, 2011

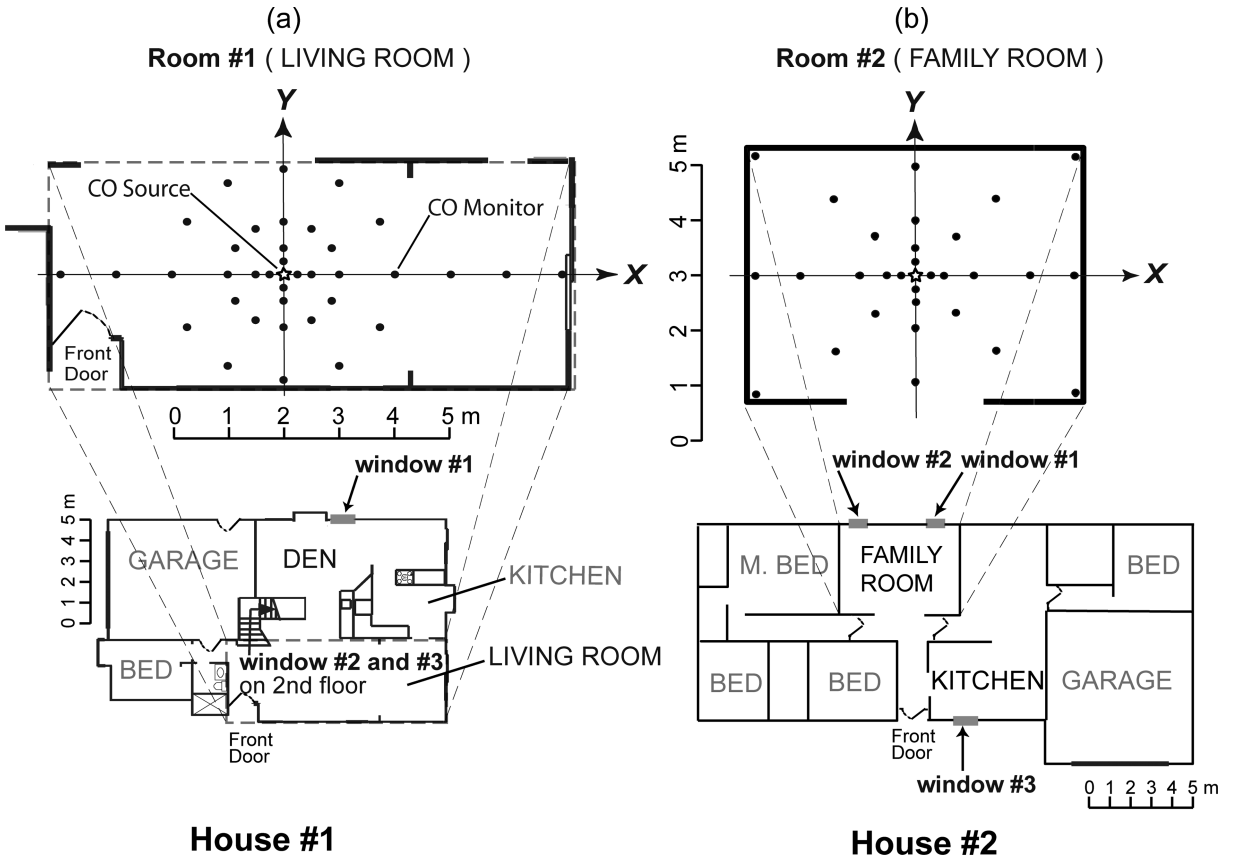

Figure 1. Plan view of CO monitoring array configurations for rooms 1 and 2 in two residential houses. The filled circles show the positions of CO monitors; the CO point source (unfilled star) is located at the intersection of the two perpendicular axes.

mechanically ventilated manufacturing facility, using an advection−diffusion model with least-squares to determine K along with three other unknowns. For an electroplating shop source, Conroy et al.[21] input 1-h-averaged concentrations at two locations into a Fick's law model to solve for K and the source emission rate. Demou et al.[22] used instantaneous measurements, along with the mass emission rate of a source, to determine K for a vehicle repair shop.

These few estimates of indoor K values have involved large occupational environments of varying size and ventilation conditions, and few monitors. With reported K values spanning 2 orders of magnitude,[26] it is difficult to select a K value for a different indoor space.

Karlsson et al.[28] derived a more general indoor turbulence dissipation model based on conservation of turbulent energy, associating K with air change rate (ACH), ventilation intake air velocity, and the temperature gradient between ceiling and floor.[23] However, the one published evaluation of this model performance found that its estimate of K was ∼60 times as high as an indoor field measurement (0.163 vs 0.0028 m^2/s), and it applies only to mechanically ventilated spaces.[22]

Our first study goal was to accurately estimate K in a type of indoor environment not previously evaluated but important for human exposure: naturally ventilated residences. A large real-time array (30−37 monitors) simultaneously monitored throughout the indoor space during continuous releases of CO. Some previous research has involved a pulse release;[7−10] we chose a continuous release to compare our residential K estimates with previous workplace estimates using a continuous source.[21,22,24] With these K values, we tested how well an isotropic eddy diffusion model can predict time-averaged concentrations at different distances from a point source inside residences.

Our second goal was to examine how air change rate and room size affect the turbulent diffusion coefficient, with the goal of exploring whether K can be estimated using parameters readily measurable in the field.

METHODOLOGY

Experimental Method. This study involved two rooms, each in a different house in northern California (Figure 1). One field site (room 1) was a 9.4 × 4.1 m living room with a single-sloped ceiling in a two-story single-family home in Redwood City, CA. The other (room 2) was a 5.6 × 4.4 m family room with a double-sloped ceiling, in a one-story ranch-style home in Watsonville, CA. In each, a point source placed at the room's center released 99.99% CO (Scott Specialty Gases, Inc., Plumsteadville, PA) at a flow rate of ∼20 cm^3 min^{-1} (∼400 μg s^{-1} at 25 °C, 1 atm), controlled by a model 5896 mass-flow controller (Emerson Electric Co., St. Louis, MO) and calibrated using a Gilibrator primary flow calibrator (Sensidyne, Inc., Clearwater, FL).

Details on the indoor tracer study are available in Acevedo-Bolton[19] Briefly, a 30-min tracer gas release duration was chosen to provide a sufficient averaging time to account for the random fluctuations of CO concentration due to indoor turbulence. This is analogous to the 10−30 min averaging times used for plume dispersion outdoors.[29] We deployed 37 (room 1) or 30 (room 2) real-time monitors (Langan Products, Inc., San Francisco, CA) surrounding the source at different radial distances and angles,

logging measurements every 15 s. Figure 1a,b shows a plan view of the two array configurations, with the source positioned at the intersection of two perpendicular axes. For each room, 16 monitors were deployed in close proximity along these two axes: four each at 0.25, 0.5, 1, and 2 m from the source. Additional monitors were placed at 1 and 2 m from the source, giving a monitor spacing of 30° for room 1, and 45° for room 2. The long (x-)axis of room 1 had two monitors each at 3 and 4 m and one at 5 m from the source. The long (x-)axis of room 2 had two monitors at 2.8 m from the source and four monitors at the corners of the room (3.56 m from the source). The source and monitors' heights were 1.0 m to approximate an adult's breathing height while sitting.

The factorial experimental design varied the number and positions of windows open for a range of natural ventilation settings (documented in Supporting Information, Table S1). The air change rate (ACH) was measured by releasing sulfur hexafluoride (SF_6) (Scott Specialty Gases, Inc., Plumsteadville, PA) for 10−20 min at the room's center at the beginning of each experiment. Two real-time SF_6 monitors (Brüel Kjær, Inc., Nærum, Denmark), placed at the two ends of the x-axis, measured SF_6 every 1 min, over ∼4 h. An indoor mass balance equation (eq 1) modeled the decreasing SF_6 concentration with time.[30]

$$C_{SF_6}(t) = C_{SF_6}(t_o)\exp(-\mathrm{ACH}(t-t_o)) \qquad \text{for } t \geq t_o \tag{1}$$

For eq 1, $C_{SF_6}(t)$ (ppm) is the SF_6 concentration at time t, and t_o (min) is the time at which SF_6 becomes well-mixed. The ACH (min^{-1}) can be found from the slope of a log−linear regression.

Two digital Hygro-Thermometers (Sunleaves Inc., Bloomington, IN) recorded temperatures near the ceiling and floor (3 m apart in room 1, 2.3 m in room 2), before and after some experiments, yielding vertical temperature gradients indicating the magnitude of indoor thermal stratification. A 2-D ultrasonic anemometer (Wind Sonic Model, Gill, Inc., Hampshire, England) placed outdoors close by recorded wind speed and direction at a 1.5 m height every 1 s.

Quality Assurance for CO Measurements. Before each experiment, the CO monitors were calibrated as described in Cheng et al.[31] The response times of these monitors were 30−50 s, giving monitoring errors <15% for averaging times >10 min under conditions with large concentration fluctuations.[31] Using the 15-s logged measurements, we computed 30-min time-averaged concentrations spanning the duration of each experiment, reducing the monitoring bias to <5%.

Characterization of Turbulent Diffusion Coefficient. To estimate the turbulent diffusion coefficient (K), we follow the widespread practice in current indoor eddy diffusion models of neglecting time-averaged indoor advection for our natural ventilation settings and invoke Fick's second law of diffusion to describe the dispersion of CO indoors. To account for the removal of CO due to air exchange during the indoor mixing process, we adopt the method developed by Drivas et al.:[23] multiplying the Fick's law solution for an instantaneous source[32] by an exponential removal term. Integrating the equation (with the exponential removal term) over time, CO concentration as a function of time, t (s), and radial distance, r (m), from our continuous source can be described as

$$C(r,t,K) = \int_0^t \frac{q}{(4\pi K t)^{1.5}}\exp\left(\frac{-r^2}{4Kt}\right)\exp(-\mathrm{ACH}\times t)\,dt \tag{2}$$

For eq 2, C ($\mu g/m^3$) is the CO concentration; q ($\mu g/s$) is the CO mass emission rate, and K (m^2/s) is an isotropic indoor turbulent diffusion coefficient. When ACH × t is sufficiently small, eq 2 can be approximated by the continuous source solution of Fick's law[32] involving an error function[33] that has been used to characterize K in different occupational workplaces.[20−22,34] On the other hand, when the time scale of air exchange (1/ACH) is comparable or less than t of interest, pollutant removal can become influential on characterized K. We evaluated the errors in using the original error function model (without removal) to predict 30-min time-averaged concentrations for different ACH and K and found errors <3% for a typical K value of 0.005 $m^2\,s^{-1}$ and for ACH < 0.5 h^{-1} (see Supporting Information, Figure S1a, b for more details).

To account for reflection of CO from wall surfaces, "*image sources*" can be introduced to the Cartesian form of eq 2 with respect to each wall plane, hypothetical sources used to satisfy no-flux boundary conditions. Drivas et al.[23] modeled air pollutant reflection from six walls of a rectangular room using an infinite series of image sources. Given our short experimental duration (30 min), we add just the six closest image sources (one for each wall) to the real source (x_o, y_o, z_o):

$$C_{\mathrm{model}}(x,y,z,t,K) = \int_0^t \frac{q\exp(-\mathrm{ACH}\times t)}{(4\pi K t)^{1.5}}\left[\exp\left(\frac{-[(x-x_o)^2+(y-y_o)^2+(z-z_o)^2]}{4Kt}\right) + \sum_{j=1}^{6}\exp\left(\frac{-[(x-x_j)^2+(y-y_j)^2+(z-z_j)^2]}{4Kt}\right)\right]dt \tag{3}$$

By defining the positions of six wall boundaries, the coordinates of the six image sources (x_j, y_j, z_j) can be determined. For the sloped ceilings in both rooms, the height for reflection is calculated as the mean of the maximum and minimum ceiling heights (4.1 m for room 1, 2.4 m for room 2).

To find the optimal isotropic K value for each experiment, a least-squares method equally weights all 30−37 of the 30-min monitor averages. The error (ε) minimized is the sum of the squared difference between each measured concentration ($\bar{C}_{\mathrm{obs}}(x_i, y_i, z_i)$) and the modeled concentration, averaged over 30 min (T).

$$\varepsilon(K) = \sum_{i=1}^{N}\left(\bar{C}_{\mathrm{obs}}(x_i,y_i,z_i) - \frac{1}{T}\int_0^T C_{\mathrm{model}}(x_i,y_i,z_i,t,K)\,dt\right)^2 \tag{4}$$

The integrations in eqs 3 and 4 were numerically approximated using the MATLAB quadrature function (*quadv*)[35] with a termination tolerance of 10^{-6}. K was estimated by minimizing eq 4, using the MATLAB nonlinear optimization function (*fminsearch*)[35] with a termination tolerance on K of 10^{-4}. We compared the value of each optimized K with that using six additional (second-nearest) image sources to verify convergence.

RESULTS AND DISCUSSION

Air Change Rate (ACH). With the exception of the 11−4−08 and 11−7−08 (night) experiments, each pair of ACH estimates was comparable and had $R^2 > 0.90$ (tabulated in the Supporting

Table 1. Turbulent Diffusion Coefficient Estimates (K) for 11 Experiments Conducted in Two Rooms at Different Air Change Rates (ACH)

	room 1					room 2					
study period	9−2−08	9−8−08	9−3−08	9−4−08	9−6−08	11−5−08	11−4−08	11−6−08 (night)	11−7−08 (night)	11−6−08	11−7−08
ACH (h^{-1})	0.17	0.51	0.57	0.78	1.25	0.19	0.37	0.41	0.59	2.08	5.40
K (m^2 s^{-1})	0.00190	0.00401[d]	0.00449	0.00515	0.00688	0.00260 (0.00107)[e]	0.00463	0.00223	0.00197	0.00684	0.0129
subplot[a]	a	b	c	d	e	f	g	h	i	j	k
m[b]	0.963	0.963	0.987	0.945	0.979	0.708 (0.754)[e]	0.996	0.956	0.898	0.944	0.899
R^2[c]	0.960	0.981	0.995	0.962	0.990	0.534 (0.704)[e]	0.983	0.944	0.857	0.907	0.817

[a] Corresponding subplot in Figure 2 for each experiment, which compares the modeled with measured dimensionless CO concentration (C/C_o) at different distances from the source. [b] Slope of the linear regression line between modeled and measured 30-min time- and radially-averaged CO concentrations at different distances from the source. [c] R^2 value of the linear regression between modeled and measured 30-min time- and radially-averaged CO concentrations at different distances from the source. [d] One CO monitor at 4 m from the source malfunctioned, so K was determined using the rest of the 36 CO monitor measurements. [e] Excludes four measurements at 0.25 m from the source.

Information, Table S2). In the 11−7−08 (night) experiment, the two ACH estimates differed by >2-fold. This was the only experiment with one widely opened window in the sampling room: monitor B was only ∼2 m from the 8-in.-opened window. For this experiment, the ACH estimate of monitor A was used for subsequent analyses.

In general, as the window openings increased, the ACH increased, ranging from 0.17 to 1.25 h^{-1} for room 1 and from 0.19 to 5.4 h^{-1} for room 2. A previous study[30] examined the effect of opening windows on ACH in two occupied residences, one of which was house 1, finding values of 0.1−3.4 h^{-1}. Our results are comparable, except for one experiment (room 2) with three wide-open windows (where ACH = 5.4 h^{-1}).

The greater ACH variation in room 2 could be due to its older construction, smaller indoor volume, and/or having open windows in the room. For two experiments with the same window settings, the two ACHs for room 1 (9−3−08, 9−8−08) were comparable (0.57, 0.51 h^{-1}), but for room 2 [11−6−08 (morning), 11−6−08 (night)] they were not (2.1, 0.4 h^{-1}). This difference could be due in part to diurnal variations: the average outdoor wind speed during the day experiment (0.9 m s^{-1}) was 1.5 times as high as during the night experiment (0.6 m s^{-1}).

Turbulent Diffusion Coefficient (K). Examples of typical time-averaged concentration distributions in the x-y plane within 2 m of the source (at the origin) were plotted using MATLAB's 2-D interpolation function (*griddata,'v4'*)[36] (Supporting Information, Figure S2a,b). The distributions were generally symmetrical around the source in both rooms. These plots support the assumption that under our natural ventilation conditions, the time-averaged advection indoors is negligible compared to turbulent diffusion. On the other hand, the concentration distribution was less symmetrical (Supporting Information, Figure S2c) for the one experimental period with a pronounced discrepancy between the two ACH estimates.

All 30−37 time-averaged CO measurements for each experiment were used, with the measured CO mass emission rate and air change rate in eq 3, to find the optimal isotropic turbulent coefficient (K). Estimates of K (Table 1) were consistent with those using six additional image sources. Compared with room 1 (K = 0.002−0.007 m^2 s^{-1}), room 2 showed K's ranging up to 0.013 m^2 s^{-1}.

Our residential K estimates are near the lower end of the wide range of reported K values (0.001−0.2 m^2 s^{-1}) for occupational indoor settings.[20−22,24] One possibility is that natural ventilation introduces less air mixing than mechanical ventilation, reducing the magnitude of turbulent mixing. In the absence of mechanical air mixing, vertical thermal stratification is also more likely, further attenuating indoor dispersion. Another possibility involves measurement scale: our array of 30−37 monitors covered the entire room, providing horizontally well-averaged estimates of K. In contrast, previous results involved a few monitors, one or a few axes, and/or shorter averaging times.

We also estimated K from selected single-direction measurements (along the positive x-direction) and using a shorter averaging time (10 min). Our resulting K values varied by two orders of magnitude. This implies that there is much greater uncertainty in estimating K when intensive spatial and temporal measurements are not available. It also indicates the difficulty of deterministically modeling concentrations over short time periods at a specific position. The model does not capture the random variations in turbulent mixing patterns, which can lead to transient directionality in the emitted plume.

Relationship between ACH and K. To examine how the measured spatial spreads of CO varied with ACH and how well the isotropic eddy diffusion model can describe the measured CO concentrations as a function of distance, we radially averaged (across all monitors at each radial distance) the 30-min time-averaged measurements. The results for each experiment were compared with the radially averaged concentrations modeled by eq 3 using the optimized K value (Table 1). Both measured and modeled concentrations (C) were then normalized by the 30-min time-averaged concentration predicted by the well-mixed mass balance model (C_o):

$$C_o = \frac{1}{T}\int_0^T \frac{q}{\mathrm{ACH}\cdot V}[1 - \exp(-\mathrm{ACH}\times t)]\,dt \qquad (5)$$

For eq 5, T is the averaging time (1800 s), q (μg/s) is the CO mass emission rate, and V (m^3) is the volume of the indoor space. Using C/C_o provided a direct comparison with the predictions of the well-mixed mass balance model.

Figure 2a−k compares the measured with the modeled dimensionless concentrations (C/C_o) for each experiment. Each column of subplots represents a room, with ACH increasing from top to bottom. Different C/C_o scales were needed for rooms 1 and 2: the emission rates used in the two rooms were comparable, but the volume of room 1 is ∼2.7 times as large as that of room 2.

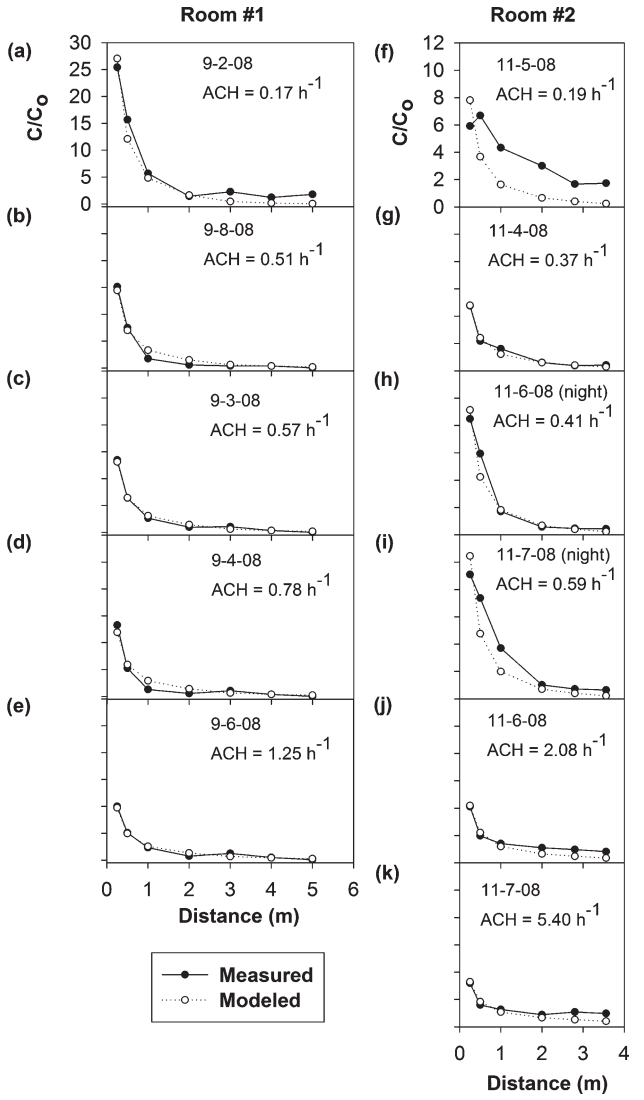

Figure 2. (a–k) Comparison between measured and modeled non-dimensionalized CO concentrations (C/C_o) for five experiments in room 1 and six experiments in room 2. The subplots for each room are stacked with increasing ACH. C is the initial 30-min time- and radially-averaged CO concentration; C_o is the initial 30-min time-averaged concentration predicted by the well-mixed mass balance model (eq 5).

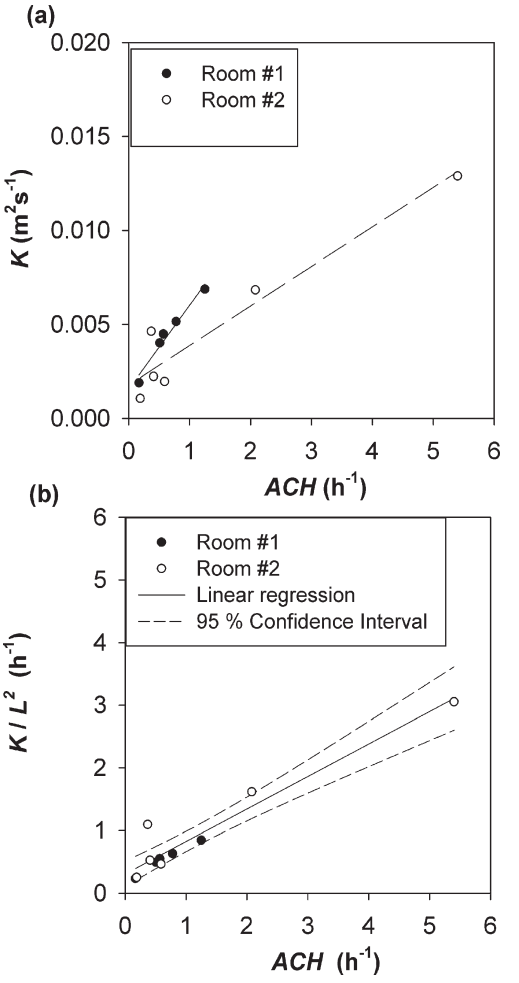

Figure 3. Associations of air change rates (ACH) with (a) turbulent diffusion coefficients (K) and (b) air mixing rates (K/L^2) for two rooms. L is the cube root of the indoor volume.

For each experiment, the measured C/C_o ratio is below 1 farthest away from the source, but above 1 for radial distances <1 m. This reflects that mixing is noninstantaneous and that background levels have not yet built up during this initial 30-min of active emissions. For both rooms, the elevation of the C/C_o ratio in close proximity to the source is least when the ACH is high.

For most experiments, the isotropic eddy diffusion model (eq 2) can describe the observed CO radial profiles with minimal error. The one exception (Figure 2f) showed lower C/C_o at 0.25 m than 0.5 m. This unusual concentration profile could reflect a time of sustained directional air motion near the source that was not well-captured by the four monitors at 0.25 m.

The strength of a linear regression between modeled and measured 30-min concentrations, radially averaged, at different distances from the source was assessed for each experiment (Table 1). Room 1 showed more consistency, with slopes (m) of 0.95–0.99 having $R^2 = 0.96–0.99$. The larger volume of room 1 and/or its indirect ventilation settings could make it less susceptible to directional air flow. For the one experiment (11–5–08, Figure 2f) with a weaker fitting result ($m = 0.71$; $R^2 = 0.53$), a second least-squares optimization excluding the 0.25 m measurements ($N = 26$) gave a lower K of 0.00107 $m^2\ s^{-1}$ ($m = 0.75$; $R^2 = 0.70$). This was used in place of the original value (0.00260 $m^2\ s^{-1}$) for subsequent analyses.

Figure 3a shows that as the ACH increased, the magnitude of K increased, with a steeper trend in room 1. In room 2, one K estimate at ACH ~ 0.5 h^{-1} was noticeably higher, deviating from the general trend. Because this was the only K in room 2 measured during an early afternoon (sunny and clear), we hypothesize that this result may reflect stronger thermally induced mixing due to incoming solar radiation, which could add to the turbulent diffusion indoors. For cases where the thermal energy input is strong while the ACH is very low, the effect of thermal mixing can become an important factor.[7]

The correlation of K for each room with the corresponding ACH is significant ($p < 0.001$), with R^2 of 0.93–0.97. However, the slope of the regression line for room 1 (solid line) is twice as large as for room 2 (dashed line). This variation could be due to the difference in volume between the two rooms (room 1 is ~2.7

times as large): while the ACH factors in the room dimensions, K does not.

To generalize between the two rooms, we defined the characteristic length scale for each room (L) as the cube root of the indoor volume (5.41 m for room 1; 3.90 m for room 2). Dividing K by L^2 yielded the same units of inverse time as ACH. K/L^2 can be thought of here as the indoor air mixing rate, the reciprocal of a time scale for turbulent mixing indoors. This formulation of the turbulent mixing time scale has been used in many water mass transfer applications (e.g., ref 37).

When the air mixing rate (K/L^2) is plotted versus ACH (Figure 3b), the trends for the two indoor spaces closely align, giving an overall significant linear correlation ($p < 0.001$, $n = 11$, $R^2 = 0.92$) with a slope of 0.52 and an intercept of 0.31 h^{-1}. Considering only the range of ACH for 95% of U.S. residences (ACH $\leq$ 2.0 h^{-1}),[38,39] we neglected the data point at ACH = 5.4 h^{-1} and found comparable regression results, but with a smaller R^2 value (slope = 0.60, intercept = 0.25 h^{-1}, $p < 0.01$, $n = 10$, $R^2 = 0.70$).

The observed linear relationship between K/L^2 and ACH is consistent with the theoretical expectation that the rate of CO loss via turbulent diffusion through opened windows is equivalent to the volume-normalized outflow rate of indoor air, ACH, based on the mass balance and scaling derivations. The positive y-intercept of the linear regression (0.31) could be associated with the thermal energy input (i.e., sunlight heating on wall surfaces) in the room further contributing to the magnitude of air mixing indoors.

Including the 95% estimated confidence interval (dashed lines) at the reported median ACH for U.S. residences (0.5 h^{-1}),[40] K/L^2 was 0.57 $\pm$ 0.17 h^{-1}. Although the levels of thermal stratification in room 1 (0.7−1.3 °F m^{-1}) were ~7 times as large as those in room 2 (0.1−0.2 °F m^{-1}), similar air mixing rate estimates were observed.

Previous studies, examining the mixing of a pulse release in an experimental room[7,8,10] and a residential bedroom and a tavern,[9] reported indoor mixing times ranging from 2 to 42 min; these were empirically based on the time required for the coefficient of variation (CV) to become <10% or <20% between monitors. Turbulent mixing time scale estimates calculated as the reciprocal of our estimated air mixing rates K/L^2 (20−260 min) are higher than these experimental mixing time values. In addition to the differences in the ventilation and experimental settings as discussed previously in the Turbulent Diffusion Coefficient section, this could be due to the different methods used to deduce mixing times; ours is a dimensional analysis approach, whereas others are based on an experimental CV criterion.

For the bedroom experiment of Klepeis[9] (ACH = 1.2 h^{-1}, L = 3 m), the turbulent mixing rate from Figure 3b yields a mixing time scale of 64 min. The corresponding K, 0.0023 m^2 s^{-1}, can be used in a pulse-release turbulent diffusion model[26] to predict concentrations as a function of time at distances of 0.5−2 m from the source. Applying the <10% CV criterion, the model's estimate of mixing time (29 min) is comparable to the published empirical value (30 min). This result suggests that the modeled K values can be used to estimate concentrations in proximity to a short- as well as a long-duration indoor source. More importantly, it demonstrates that the empirical relationship between K/L^2 and ACH (Figure 3b) can reliably characterize the rate of pollutant mixing in another naturally ventilated room.

IMPLICATIONS

The reasonable agreement between modeled and measured average concentrations in two residences shows that currently available indoor turbulent diffusion models can predict average exposures in close proximity to emitting sources inside naturally ventilated spaces, as long as the turbulent diffusion coefficient (K) can be estimated. The significant linear correlation found in this study between the indoor air mixing rate (K/L^2) and the air change rate suggests that human exposure investigators can reasonably estimate the indoor turbulent diffusion coefficient in many field settings, by measuring just the air change rate and indoor dimensions of the space.

A number of studies have shown that higher concentrations and exposures occur near actively emitting indoor air pollutant sources ranging from smoking and cooking to household cleaning.[11−14,16−19] However, no previously published model for residential environments has offered physics-based insights regarding the proximity effect. While the relationship between turbulent diffusion and pollutant distribution indoors is complex, we believe this model represents a significant step toward understanding a major factor that affects the indoor proximity effect.

ASSOCIATED CONTENT

Supporting Information. The factorial design, with window openings for each experiment (Table S1), and the air change rate (ACH) (Table S2); errors of the original error function model for different ACH (Figure S1); and three examples of horizontal CO distributions measured indoors (Figure S2). This material is available free of charge via the Internet at http://pubs.acs.org.

AUTHOR INFORMATION

Corresponding Author
*E-mail: kccheng78@gmail.com.

ACKNOWLEDGMENT

This research was supported by a grant from the Tobacco-Related Disease Research Program (TRDRP, Oakland, CA). The authors thank Lee Langan of Langan Products, Inc. for advice on the operation and calibration of CO monitors.

REFERENCES

(1) Shair, F. H.; Heitner, K. L. Theoretical model for relating indoor pollutant concentrations to those outside. *Environ. Sci. Technol.* **1974**, *8*, 444–451.

(2) Hayes, S. R. Use of an indoor air quality model (IAQM) to estimate indoor ozone levels. *J. Air Waste Manage. Assoc.* **1991**, *41*, 161–170.

(3) Keil, C. B. The development and evaluation of an emission factor for toluene parts-washing process. *Am. Ind. Hyg. Assoc. J.* **1998**, *59*, 14–19.

(4) Burke, J. M.; Zufall, M. J.; Özkaynak, H. A population exposure model for particulate matter: Case study results for PM2.5 in Philadelphia, PA. *J. Exposure Anal. Environ. Epidemiol.* **2001**, *11*, 470–489.

(5) Ott, W. R.; Klepeis, N. E.; Switzer, P. Analytical solutions to compartmental indoor air quality models with application to environmental tobacco smoke concentrations measured in a house. *J. Air Waste Manage. Assoc.* **2003**, *53*, 918–936.

(6) Vernez, D.; Bruzzi, R.; Kupferschmidt, H.; De-Batz, A.; Droz, P.; Lazor, R. Acute respiratory syndrome after inhalation of waterproofing sprays: A posteriori exposure-response assessment in 102 cases. *J. Occup. Environ. Hyg.* **2006**, *3*, 250–261.

(7) Baughman, A. V.; Gadgil, A. J.; Nazaroff, W. W. Mixing of a point source pollutant by natural convection flow within a room. *Indoor Air* **1994**, *4*, 114–122.

(8) Drescher, A. C.; Lobascio, C.; Gadgil, A. J.; Nazaroff, W. W. Mixing of a point source indoor pollutant by forced convection. *Indoor Air* **1995**, *5*, 204–214.

(9) Klepeis, N. E. Validity of the uniform mixing assumption: Determining human exposure to environmental tobacco smoke. *Environ. Health Persp.* **1999**, *107* (Suppl. 2), 357–363.

(10) Jones, R.; Nicas, M. Experimental determination of supermicrometer particle fate subsequent to a point release within a room under natural and forced mixing. *Aerosol Sci. Technol.* **2009**, *43*, 921–938.

(11) Rodes, C.; Kamens, R.; Wiener, R. The significance and characteristics of the personal activity cloud on exposure assessment measurements for indoor contaminants. *Indoor Air* **1991**, *2*, 123–145.

(12) Furtaw, J.; Pandian, M. D.; Nelson, D. R.; Behar, J. V. Modeling indoor air concentrations near emission sources in imperfectly mixed rooms. *J. Air Waste Manage. Assoc.* **1996**, *46*, 861–868.

(13) McBride, S. J.; Ferro, A.; Ott, W. R.; Switzer, P.; Hildemann, L. M. Investigations of the proximity effect for pollutants in the indoor environment. *J. Exposure Anal. Environ. Epidemiol.* **1999**, *9*, 602–621.

(14) McBride, S. J. A marked point process model for the source proximity effect in the indoor environment. *J. Am. Stat. Assoc.* **2002**, *97*, 683–691.

(15) Ott, W. R.; McBride, S. J.; Switzer, P. In *Indoor Air '02, Proceedings of the Eighth International Conference on Indoor Air Quality and Climate.*; Levin, H., Ed.; Monterey, CA, 2002; Vol. 4, pp 229−234.

(16) Ferro, A. R.; Hildemann, L. M.; McBride, S. J.; Ott, W. R.; Switzer, P. In *Air Pollution VII*; Brebbia, C. A., Jacobson, M., Power, H., Eds.; WIT Press: Southampton, UK, 1999; pp 487−496.

(17) Ferro, A. R.; Kopperud, R. J.; Hildemann, L. M. Elevated personal exposure to particulate matter from human activities in a residence. *J. Exposure Anal. Environ. Epidemiol.* **2004**, *14*, S34–S40.

(18) Ferro, A. R.; Klepeis, N. E.; Ott., W. R.; Nazaroff, W. W.; Hildemann, L. M.; Switzer, P. Effect of interior door position on room-to-room differences in residential pollutant concentrations after short-term releases. *Atmos. Environ.* **2009**, *43*, 706–714.

(19) Acevedo-Bolton,V. *Characterizing personal exposure in close proximity to indoor air pollution sources*. Ph.D. Dissertation, Stanford University, Stanford, CA, 2010; Chapter 2.

(20) Wadden, R. A.; Scheff, P. A.; Franke, J. E. Emission factors for trichloroethylene vapor degreasers. *Am. Ind. Hyg. Assoc. J.* **1989**, *50*, 496–500.

(21) Conroy, L. M.; Wadden, R. A.; Scheff, P. A.; Franke, J. E.; Keil, C. B. Workplace emission factors for hexavalent chromium plating. *Appl. Occup. Environ. Hyg.* **1995**, *10*, 620–627.

(22) Demou, E.; Hellweg, S.; Wilson, M. P.; Hammond, S. K.; McKone, T. E. Evaluating indoor exposure modeling alternatives for LCA: A case study in the vehicle repair industry. *Environ. Sci. Technol.* **2009**, *43*, 5804–5810.

(23) Drivas, P. J.; Valberg, P. A.; Murphy, B. L.; Wilson, R. Modeling indoor air exposure from short-term point source releases. *Indoor Air* **1996**, *6*, 271–277.

(24) Scheff, P. A.; Friedman, R. L.; Franke, J. E.; Conroy, L. M.; Wadden, R. A. Source activity modeling of Freon emissions from open-top vapor degreasers. *Appl. Occup. Environ. Hyg.* **1992**, *7*, 127–134.

(25) Jayjock, M. A.; Chaisson, C. F.; Arnold, S.; Dederick, E. J. Modeling framework for human exposure assessment. *J. Expo. Sci. Environ. Epidemiol.* **2007**, *17*, S81–S89.

(26) Nicas, M. In *Mathematical Models for Estimating Occupational Exposure to Chemicals*, 2nd ed., AEAM09−379; Keil, C. B., Simmons, C. E., Anthony, T. R., Eds.; AIHA Press: Fairfax, VA, 2009; pp 53−65.

(27) Nicas, M. Modeling turbulent diffusion and advection of indoor air contaminants by Markov chains. *Am. Ind. Hyg. Assoc. J.* **2001**, *62*, 149–158.

(28) Karlsson, E.; Sjostedt, A.; Hakansson, S. Can weak turbulence give high concentrations of carbon dioxide in baby cribs? *Atmos. Environ.* **1994**, *28*, 1297–1300.

(29) Gifford, F. A. Use of routine meteorological observations for estimating atomospheric dispersion. *Nucl. Saf.* **1961**, *2*, 47–51.

(30) Howard-Reed, C.; Wallace, L. A.; Ott, W. R. The effect of opening windows on air change rates in two homes. *J. Air Waste Manage. Assoc.* **2002**, *52*, 147–159.

(31) Cheng, K. C.; Acevedo-Bolton, V.; Jiang, R. T.; Klepeis, N. E.; Ott, W. R.; Hildemann, L. M. Model-based reconstruction of the time response of electrochemical air pollutant monitors to rapidly varying concentrations. *J. Environ. Monitor* **2010**, *12*, 846–853.

(32) Crank, J. *The Mathematics of Diffusion*; Oxford University Press Inc.: New York, 1975; pp 29−32.

(33) Charbeneau, R. J. *Groundwater Hydraulics and Pollutant Transport*; Prentice-Hall, Inc.: Upper Saddle River, NJ, 2000; pp 546−549.

(34) Bennett, J. S.; Feigley, C. E.; Khan, J.; Hosni, M. H. Comparison of emission models with computational fluid dynamic simulation and a proposed improved model. *Am. Ind. Hyg. Assoc. J.* **2003**, *64*, 739–754.

(35) Palm, W. J. *Introduction to Matlab 7 for Engineers*; McGraw-Hill: New York, 2005; pp 161−162, 472−477.

(36) Trauth, M. H. *MATLAB Recipes for Earth Sciences*; Springer: New York, 2007; pp 164−172.

(37) Fischer, H. B.; List, E. J.; Imberger, J.; Koh, R. C. Y.; Brooks, N. H. *Mixing in Inland and Coastal Waters*; Academic Press: New York, 1979, p 13.

(38) Wilson, A. L.; Colome, S. D.; Tian, Y.; Becker, E. W.; Baker, P. E.; Behrens, D. W.; Billick, I. H.; Garrison, C. A. California residential air exchange rates and residence volumes. *J. Exposure Anal. Environ. Epidemiol.* **1996**, *6*, 311–326.

(39) Pandian, M. D.; Behar, J. V.; Ott, W. R.; Wallace, L. A.; Wilson, A. L.; Colome, S. D.; Koontz, M. Correcting errors in the nationwide data base of residential air exchange rates. *J. Exposure Anal. Envon. Epidemiol.* **1998**, *8*, 577–585.

(40) Murray, D. M.; Burmaster, D. E. Residential air exchange rates in the United States: Empirical and estimated parametric distributions by season and climatic region. *Risk Anal.* **1995**, *15*, 459–465.